Journal of Thermal Analysis and Calorimetry (2018) 132:835–842
https://doi.org/10.1007/s10973-018-6976-6

Analysis and characterization of the transition from the Arrhenius to non-Arrhenius structural relaxation in fragile glass-forming liquids

Masahiro Ikeda[1] · **Masaru Aniya**[2]

Received: 7 September 2017 / Accepted: 5 January 2018 / Published online: 27 January 2018

Abstract
We have studied the transition from an Arrhenius-like to a non-Arrhenius-like structural relaxation behavior in fragile glass-forming liquids. This transition is denoted by the temperature T_A that usually occurs above the melting point T_m and the dynamic crossover temperature T_B. Recent studies reveal that T_A is a characteristic temperature related with the dynamical properties of the system. However, its unambiguous determination is not easy. In this work, a method to obtain the temperature T_A from the experimental data of α-relaxation time is presented. The obtained T_A is compared with the cooperativity onset temperature T_x extracted from the bond strength–coordination number fluctuation model. The result reveals that T_A is close to T_x for fragile liquids. From the result of the present analyses combined with the linear relation $T_x \propto T_0$, where T_0 is the Vogel temperature, the Arrhenius crossover phenomenon in fragile liquids is linked to the low-temperature structural relaxation dynamics.

Keywords Arrhenius crossover · Cooperativity onset temperature · Ideal glass-transition temperature

Introduction

Fragility is one of the key parameters used in the understanding of fundamental property of glass-forming materials [1–3]. It quantifies how sharply the relaxation time or the viscosity changes near the glass-transition temperature T_g. However, at temperature much higher than T_g, or even above the dynamic crossover temperature T_B [4–6], there is an indication of the existence of a phenomenon closely related to the fragility which is involved in the glass transition. The temperature dependence of the α relaxation time [7–9] and the transport coefficients such as viscosity [10, 11] and diffusivity [12, 13] exhibits an Arrhenius-like pattern at high temperature and transforms to a non-Arrhenius-like one at lower temperature. This transition which is denoted by T_A is called Arrhenius temperature [14] (or Arrhenius crossover temperature [12]). Below T_A, the cooperative relaxation or the dynamic heterogeneity grows markedly. For good glass formers, this type of transition occurs above the melting point T_m [15]. Interestingly, it has been reported [12, 14] that the characteristic temperature ratio T_A/T_g is correlated with the fragility index m. From these observations, one expects that the properties of glassy materials can be understood through the knowledge of the transition from the Arrhenius-like relaxation regime in the liquid state. However, the relationship between the high-temperature transition occurring at T_A and the low-temperature relaxation occurring near T_g is not fully explored.

For typical fragile glass-forming liquids, T_A/T_g spans roughly between unity and about 2, depending on the nature of the materials. For example, for molecular liquids, the temperature ratio is in the range $T_A/T_g \approx 1.4$–2.1 [14, 15]. For metallic systems, it is found universally that $T_A/T_g \approx 2$ [12, 13]. For network glass formers, in contrast to the above fragile systems, the ratio spreads in a broader range $T_A/T_g \approx 1.6$–4 [12]. It should be also kept in mind that there is a certain difficulty in identifying the characteristic temperatures T_A and T_g. Usually, T_g is determined

✉ Masahiro Ikeda
mikeda@hotmail.co.jp

[1] Department of General Education, National Institute of Technology, Oita College, 1666, Maki, Oaza, Oita 870-0152, Japan

[2] Department of Physics, Faculty of Advanced Science and Technology, Kumamoto University, Kumamoto 860-8555, Japan

from calorimetric measurements [16–18], or conveniently by the temperature at which the relaxation time reaches $\tau = 100$ s. However, the value of τ (T_g) could depend to some extent on the materials. Other methods to determine T_g experimentally have been proposed (for instance, Ref. [18]). According to Popova et al. [7], the transition of the structural relaxation from an Arrhenius-like to a non-Arrhenius-like behavior can be described by either, a continuous or a discontinuous function. This is a question of fundamental importance in the study of dynamic crossover phenomena in glass-forming liquids, since the latter implies that a phase transition occurs at T_A [7]. However, the high-temperature transition from an Arrhenius-like behavior to a non-Arrhenius-like one is seen as a quite continuous variation [8–11, 13, 19]. If the transition happens suddenly as described by the Arrhenius equation to the Vogel–Fulcher–Tammann (VFT) equation, it should be observed in a narrow temperature range about 15 K [7]. Besides, the Arrhenius-like behavior does not necessarily guarantee a true Arrhenius law up to the high-temperature limit. Actually, in ionic liquids, a quite slightly curved behavior was observed [20] in the structural relaxation time around the Arrhenius crossover region. Particularly above the boiling point T_b, careful consideration should be given in the interpretation to the behavior [21].

In our recent study [22], we reported that the bond strength–coordination number fluctuation (BSCNF) model [23–25], which was originally proposed to explain the viscosity behaviors [23], is applicable to the temperature dependence of the non-Arrhenius structural relaxation time with an Arrhenius-like behavior at high temperature. There, it was found [22] that the analysis of the cooperative relaxation based on the BSCNF model enables to extract the characteristic temperature T_x. It was also shown that T_x takes a value close to T_A for the fragile liquids investigated. The expression of T_x given in the next section provides a way to demarcate the high-temperature relaxation regime into less cooperative process and apparent cooperative one. If we assume that T_x is closely associated with T_A, some implications on Arrhenius crossover phenomena can be obtained. For instance, upon cooling the growth degree of cooperativity becomes prominent around T_x due to the formation of strong coupling between nearest-neighbor molecular units. This picture derived from the BSCNF model is compatible with the idea of short-range bond ordering in liquids that emerges at T_A as pointed out by Surovtsev [15]. From such considerations, we have considered T_x to be a characteristic temperature that describes the cooperativity onset at high-temperature region. This suggests the possibility that the Arrhenius crossover phenomenon can be understood from a viewpoint based on the BSCNF model. In order to confirm this, it is necessary to determine directly both T_A and T_x for various glass-forming liquids.

In this study, we investigated the two characteristic temperatures T_A and T_x of propylene carbonate (PC) and ethanol. To verify the applicability of the BSCNF model, the result of 2-methyl tetrahydrofuran (MTHF) is also presented for comparison. The experimental data analyzed in the present study are taken from the literatures [8, 9, 19, 26]. The data are also used to confirm the T_A of the materials considered. In particular, in the present study, a new method of analysis is introduced to determine T_A by paying attention to the variation in the averaged slope angle $\Delta\bar{\phi}(T)$. Here, $\phi(T)$ is the slope angle defined in Eq. (9) that is obtained from the inverse temperature derivative of the logarithm of relaxation time. The novel method used in the evaluation of $\phi(T)$ permits to extract the Arrhenius crossover characteristics. The result obtained is discussed along with our recent study [22]. There, it is discussed how the high-temperature transition from the Arrhenius-like relaxation behavior in fragile glass-forming liquids can be linked to the low-temperature relaxation dynamics in terms of the BSCNF model.

Characterization of the transition from the Arrhenius-like to the non-Arrhenius-like behavior

Cooperativity onset temperature T_x

In recent years, the Arrhenius crossover phenomena have been found in different glass-forming materials, and its mechanisms have been studied. For instance, for metallic glass-forming systems, molecular dynamics simulations [13, 27] and quasi-elastic neutron scattering measurements [27] have revealed that the Stokes–Einstein law is violated markedly below T_A. From a fundamental aspect, Surovtsev et al. [9, 15] have discussed the origin of the high-temperature transition from the Arrhenius-like behavior to the non-Arrhenius-like one and further evidenced it by their experimental results [28]. According to their study [15], the temperature ratio T_A/T_m can be a useful indicator to access the glass-forming ability. For instance, for good glass formers, the short-range bond ordering incompatible with the long-range order substantially prevents the crystallization. In this case, the temperature ratio T_A/T_m takes a value larger than 1.0. In this regard, Surovtsev et al. have interpreted T_A as the initiation temperature where a locally favored structure or the nanometer-scale structure is formed in the high-temperature liquid state [9, 15].

According to the BSCNF model [22, 23], the temperature dependence of the structural relaxation time τ is given by

$$\tau = \frac{\tau_0}{\sqrt{1-Bx^2}} \exp\left(\frac{Cx + CH(B,C)x^2}{1-Bx^2}\right), \quad (1)$$

where

$$H(B,C) = \left\{\ln\left(\frac{\tau_{T_g}}{\tau_0}\right) + \frac{1}{2}\ln(1-B)\right\}\frac{(1-B)}{C} - 1, \quad (2)$$

$$B = \frac{(\Delta E)^2(\Delta Z)^2}{R^2 T_g^2} \quad \text{and} \quad C = \frac{E_0 Z_0}{RT_g}, \quad (3)$$

where x is the inverse temperature normalized by T_g, i.e., $x = T_g/T$. E_0 and Z_0 are the mean value of the bond strength and the coordination number of the structural units that form the melt, and ΔE and ΔZ are their fluctuation, respectively. τ_0 is the relaxation time at the high temperature limit. Recently, it was shown [22] that from the analysis of temperature dependence of molecular cooperativity in the light of the BSCNF model, the high-temperature relaxation regime can be characterized by the temperature T_x,

$$\frac{T_x}{T_g} = \left(\frac{B}{\sqrt{5}-2}\right)^{1/2}, \quad (4)$$

where B is one of the BSCNF model parameters given in Eq. (3). For the fragile glass formers investigated, T_x/T_g was found to be $T_x/T_g \approx 1.6$–1.8 [22]. It is interesting to note that for fragile liquids, this value is close to T_A/T_g (≈ 1.5–2.0) [15] and obviously higher than T_B/T_g (≈ 1.2–1.3) [4–7]. Furthermore, it is also worthwhile noting that T_x is written in terms of B. That is, T_x is associated with the degree of fluctuations in bond energy E and coordination number Z. Indeed, Eq. (4) is derived from the temperature-dependent number of structural unit N_B defined as

$$N_B = \frac{E_\tau}{E_0 Z_0}, \quad (5)$$

where E_τ is the activation energy for the structural relaxation, and $E_0 Z_0$ is the average binding energy per structural unit. Hence, N_B gives the number of structural units involved when a structural unit is broken apart and moves from one position to another. The BSCNF model estimates that for fragile polymeric materials, N_B grows up to approximately an order of 100 at the glass transition range [22, 29]. This is comparable to the cooperativity evaluated by the Donth formula which is based on quantities determined from calorimetric measurements [16, 17, 30–32]. In this work, we focus mainly in the high-temperature relaxation property. What matters here is that the values of N_B at T_x were found to be about $N_B(T_x) \sim 2$ [22], which suggests the followings: The transition from the Arrhenius-like behavior to the non-Arrhenius-like one begins when about two molecular units are coupled, and such molecular coupling results from the formation of strong bonds between particular molecular units. These pictures derived theoretically motivated us to perform the present study and consider the underlying factors that exist behind the Arrhenius crossover phenomenon.

Analysis based on the variation of the averaged slope angle $\Delta\bar{\phi}(T)$

The determination of T_A from the temperature dependence of the structural relaxation time data is not simple, because for a number of fragile liquids the Arrhenius crossover appears quite continuously. In most relevant studies, analytical methods based on the temperature-derivative analysis [19] have been widely used to specify the dynamic crossover points above the glass-transition temperature [6, 7, 9, 33–35]. The temperature-derivative analysis is based in the following expression (which is the Stickel plot)

$$f_\tau(T) = \left(\frac{\mathrm{d}\ln\tau}{\mathrm{d}(1/T)}\right)^{-1/2}. \quad (6)$$

Equation (6) gives a clear profile on how sensitive the non-Arrhenius relaxation time is to temperature variations. In particular, Eq. (6) is effective when it is used together with both, the Arrhenius equation and the VFT equation. When the Arrhenius equation $\tau = \tau_0 \exp(E_\infty/RT)$ is applied to Eq. (6), the Stickel plot $f_\tau(T)$ becomes independent of temperature,

$$\left(\frac{\mathrm{d}\ln\tau^{(\mathrm{Arrhenius})}}{\mathrm{d}(1/T)}\right)^{-1/2} = \left(\frac{E_\infty}{R}\right)^{-1/2} = \text{const}, \quad (7)$$

where E_∞ and R are the activation energy and the gas constant, respectively. While the VFT equation $\tau = \tau_0 \exp[B_{VFT}/(T - T_0)]$ is used in Eq. (6), the following linearized equation is obtained,

$$\left(\frac{\mathrm{d}\ln\tau^{(\mathrm{VFT})}}{\mathrm{d}(1/T)}\right)^{-1/2} = \left(1 - \frac{T_0}{T}\right)\frac{1}{\sqrt{B_{VFT}}}. \quad (8)$$

By using the above method, T_A is determined unambiguously from the intersection of Eqs. (7) and (8) [7, 9]. However, one encounters a difficulty in the analysis based on derivation, in particular when the experimental discrete data are directly used [7]. Therefore, when the experimental data set is applied to Eq. (6), additional operation is needed to smooth out the behavior of $f_\tau(T)$. Without such an operation, the feature of the transition across T_A is not unambiguously determined from the temperature-derivative profile. For instance, in Ref. [7], a temperature interval

ΔT (= 8 K) is used to smooth out the discrete data set. Otherwise, the use of smaller ΔT (than 8 K) makes the profile poorly highlighted, and in such a case the data points become scattered. As a result, the profile turns out obscure.

In the temperature range lower than T_A, Eq. (6) is used so far to evaluate the deviation from the linear relation given by Eq. (8). The deviation indicates the inadequacy of using a single VFT equation [6, 19, 35]. In such cases, additional VFT expressions are needed to account for the experimental results. Often, a switching to another VFT-like behavior is detected around T_B, and such crossover points are found to be close to the mode-coupling temperature T_{MCT} [4, 36] and the α–β bifurcation temperature T_β [37]. In one of our previous works [38], we studied the critical temperature T_c for a family sample of unsaturated polyester resins [39] by using the random-walk (RW) model proposed by Arkhipov and Bässler [40]. According to the RW model, T_c demarcates the structural relaxation regime between a non-cooperative relaxation process and a cooperative one. The result was that T_c took a value of about 1.04–1.06T_g, which is rather lower than T_B and T_A. In Table 1, the reported values of T_B for the materials under consideration are indicated. From a fundamental point of view, it is of paramount importance to extract meaningful information about pre-vitrification of a liquid from the crossover temperatures and the dynamic properties. The crossover temperatures mentioned above enable the characterization of glass-forming liquids. These temperatures separate in their own way the liquid relaxation regime into a non-cooperative process and a cooperative one. Meanwhile, the Arrhenius crossover behavior is a salient change in the temperature dependence of the structural relaxation. It suggests a shift from a simple thermally activated law to a more complex law reflecting the many-body interactions in glass-forming liquids [41], which can be modeled theoretically [8, 9, 42, 43]. However, before theoretic modeling, clear characterization of such a change occurring at high-temperature region is necessary.

In what follows, we present an analytical method for evaluating T_A from the α-relaxation time data. Specifically, the analytical method is based on the variation in the averaged slope angle $\Delta\bar{\phi}(T)$, where ϕ is the slope angle defined as

$$\phi(T) = \tan^{-1}\left(\frac{\mathrm{d}\log_{10}\tau}{\mathrm{d}(10^3/T)}\right). \tag{9}$$

It is noted here that $\phi(T)$ is similar to Eq. (6) in the point that it is based on the temperature derivation. Despite the similarity, Eq. (9) enables to capture through the slope angle the gradual and continuous change in the curvature of $\log(\tau/\mathrm{s})$ around the transition point, by using the averaging operation explored in the present study. The schematic illustration of the present method is shown in Fig. 1a–c. Here, (a) is an illustration of the definition of $\phi(T)$ and its initial value ϕ_0, (b) is obtained from the averaging operation, and (c) is the outline of the present method. In practice, we examine the difference between $\phi(T)$ and ϕ_0

$$\Delta\phi(T) = \phi(T) - \phi_0, \tag{10}$$

where ϕ_0 is the slope angle that corresponds to E_∞ of the Arrhenius-like relaxation behavior at high temperatures. Regarding the procedure for smoothing the discrete data points, we employ the averaging operation as follows.

Firstly, as we can see from the inset in Fig. 1b, $d\log_{10}(\tau/\mathrm{s})/dy$ is approximated by $\Delta\log_{10}(\tau/\mathrm{s})/\Delta y$, where y is $1000/T$. The new point of our method rests in the way of taking the average over the data points. As shown in Fig. 1b, we carry out the averaging operation twice in the entire temperature range of the data points. In the first averaging operation denoted by $\bar{\phi}_+(T)$, more $\Delta\log_{10}(\tau/\mathrm{s})/\Delta y$ data points in the higher temperature side are taken. An example is shown in Fig. 1b. In this example, at temperature denoted by full circle, the average $\bar{\phi}_+(T)$ is obtained by using 7 data points at the high-temperature side and 2 points at the low-temperature side. As is clearly seen from Fig. 1b, this type of

Table 1 Parameters of fragile glass-forming liquids investigated in the present study

Material	E_∞/kJmol^{-1}	$\ln(\tau_0/\mathrm{s})$	$\ln(\tau_{Tg}/\tau_0)$	B	C	T_x/K	T_A/K	T_B/K	T_g/K	References
Propylene carbonate (PC)	11.8	− 25.7	29.2	0.785	4.44	292	286, 290[a]	194	160	[6, 9, 15, 19, 44]
Ethanol	26.5	− 16.0	39.0	0.706	19.6	208	186, 213[a], 167[a]	111	99	[6, 14, 15, 26]
2-Methyl tetrahydrofuran (MTHF)	9.4	− 29.8	31.6	0.750	7.95	165	189[a]	115	92	[6, 8]

The values of T_A with [a] indicate the reported value in other studies, otherwise, are obtained from the present analyses. T_x is obtained from Eq. (4) with B determined in the analyses of Fig. 4. For the analysis of MTHF, we have used the reference temperature $T_g = 120$ K corresponding to $\tau = 100$ s in place of $T_g = 92$ K [26]. The dynamic crossover temperatures T_B are taken from Ref. [6]

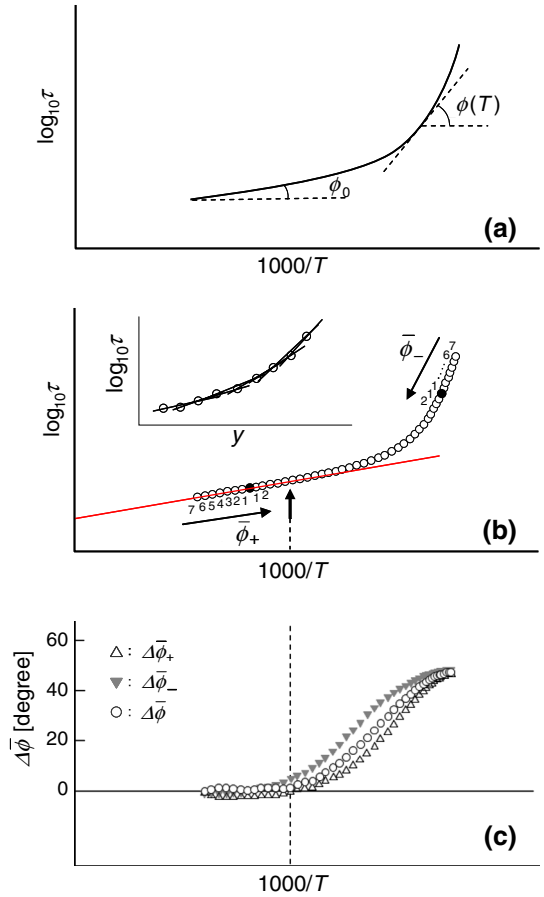

Fig. 1 **a** Slope angle $\phi(T)$ defined in Eq. (9) and the initial value ϕ_0 beginning at the highest-temperature data point. **b** Averaging operations $\Delta\bar{\phi}_+(T)$ and $\Delta\bar{\phi}_-(T)$, where the deviation $\Delta\bar{\phi}(T)$ follows Eq. (10). The inset indicates that $d\log_{10}(\tau/\mathrm{s})/dy$ is approximated by $\Delta\log_{10}(\tau/\mathrm{s})/\Delta y$, where y is $1000/T$. **c** Geometric average of $\Delta\bar{\phi}_+(T)$ and $\Delta\bar{\phi}_-(T)$ as given by Eq. (11)

operation emphasizes the Arrhenius-type behavior observed at high temperatures. On the other hand, in the second averaging process denoted by $\bar{\phi}_-(T)$, more data points at the lower-temperature side around a certain temperature (denoted as full circle) are included therein (2 data points at the high-temperature side and 7 points at the low-temperature side). Contrary to $\bar{\phi}_+(T)$, this type of operation emphasizes the non-Arrhenius-type behavior at lower temperatures. In the above method, the characteristics at the higher- and lower-temperature regions are reflected in $\bar{\phi}_+(T)$ and $\bar{\phi}_-(T)$, respectively. In order to describe the change of $\phi(T)$ over the whole range of structural relaxation, including the intermediate temperature range, we subtract ϕ_0 from both $\bar{\phi}_+(T)$ and $\bar{\phi}_-(T)$ and take the geometric average as

$$\Delta\bar{\phi}(T) = \sqrt{|\Delta\bar{\phi}_+||\Delta\bar{\phi}_-|}. \tag{11}$$

The behaviors of $\Delta\bar{\phi}_+(T)$, $\Delta\bar{\phi}_-(T)$, and $\Delta\bar{\phi}(T)$ are shown in Fig. 1c. As mentioned above, the keypoint of the present method is that $\Delta\bar{\phi}_+(T)$ includes more information on high-temperature slopes reflected in the Arrhenius-like patterns and less information on lower temperature slopes, simultaneously. On the other hand, $\Delta\bar{\phi}_-(T)$ reflects heavily the lower temperature slopes of the non-Arrhenius-like pattern than the Arrhenius-like one. Thus, the geometric value calculated from Eq. (11) compensates the lack of information of $\Delta\bar{\phi}_+(T)$ and $\Delta\bar{\phi}_-(T)$, which enables to obtain the Arrhenius crossover characteristics across the transition.

Results and discussion

Figure 2 shows the results of the analysis for PC, where the temperature dependence of $\log_{10}(\tau/\mathrm{s})$, $\Delta\bar{\phi}(T)$, and f_τ (T) converted from $\bar{\phi}(T)$ are shown in (a), (b), and (c), respectively. In the upper figure (a), the Arrhenius behavior (solid red line) with the activation energy E_∞ is described by using the value ϕ_0. The blue curve on the experimental

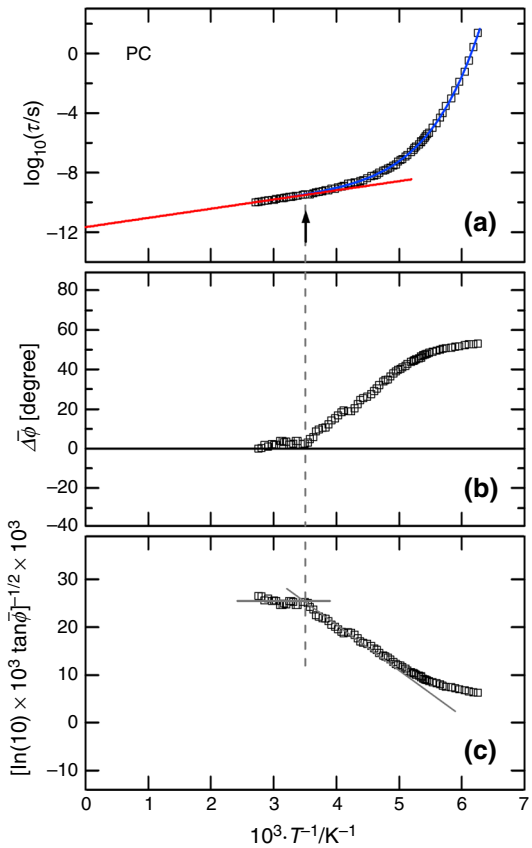

Fig. 2 Temperature dependence of **a** $\log_{10}(\tau/\mathrm{s})$, **b** $\Delta\bar{\phi}(T)$ and **c** f_τ (T) converted from $\bar{\phi}(T)$ for PC. In **b**, $\Delta\bar{\phi}(T)$ is plotted with Eq. (11) multiplied by $180/\pi$. The arrow in (**a**) and the vertical dashed lines in (**b**) and **c** denote the transition point T_A. The used data are taken from refs. [9, 19, 44]

data at low temperatures is simply calculated from a polynomial fitting function, which is indicated to see the deviation from the Arrhenius behavior. In the middle figure (b), we can see in $\Delta\bar{\phi}(T)$ the appearance of a bend that specifies T_A of the present analysis. The location of the temperature T_A is denoted by an up-pointing arrow in figure (a) and by vertical dashed lines in figures (b) and (c). From the analyses, we obtain $T_A = 286$ K for PC, which agrees with the reported $T_A^* = 290$ K [9, 15], but is slightly lower than 300 K reported in Ref. [19]. In figure (c), the vertical scale is given by $[\ln(10) \times 10^3 \tan\bar{\phi}]^{-1/2} \times 10^3$ that corresponds to $f_\tau\ (T) \times 10^3$. Here, the horizontal and the linear lines with a negative slope are described in the same way to Eqs. (7) and (8), respectively. The intersection of the two straight lines coincides with the location of the arrow in Fig. 2a.

Figure 3 shows the results of the analysis for ethanol, and the figures (a), (b), and (c) are analogous to those of Fig. 2. Here, Fig. 3a shows that compared to PC, the temperature dependence of $\log_{10}(\tau/s)$ exhibits a clearer Arrhenius-like behavior owing to its higher value of E_∞. The experimental data are taken from Ref. [26].

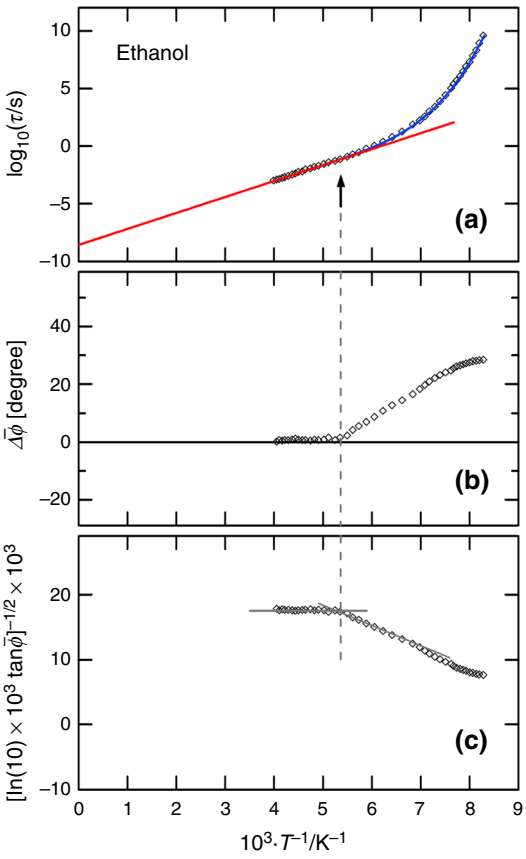

Fig. 3 Temperature dependence of **a** $\log_{10}(\tau/s)$, **b** $\Delta\bar{\phi}(T)$ and **c** $f_\tau(T)$ for ethanol. The explanations of the figures are the same to that in Fig. 2. The experimental data used are taken from Ref. [26]

Accordingly, $\Delta\bar{\phi}(T)$ exhibits a clear bend, from which we obtain $T_A = 186$ K. However, different values of T_A for ethanol are reported, e.g., 213 K [9] and 167 K [14]. The Arrhenius temperature T_A obtained here takes an intermediate value between these values.

Figure 4 shows the temperature dependence of the structural relaxation data of PC, ethanol and MTHF fitted with Eq. (1), which is the main result of the present work. As we can see from Fig. 4, the BSCNF model describes reasonably well the experimental data in a wide temperature range. In particular, it can be observed that Eq. (1) is able to describe the Arrhenius-like behavior at the high-temperature region. It is noted, however, that the behavior of Eq. (1) above T_x is not a straight line that extends to the high-temperature limit. At higher temperature than T_x, the

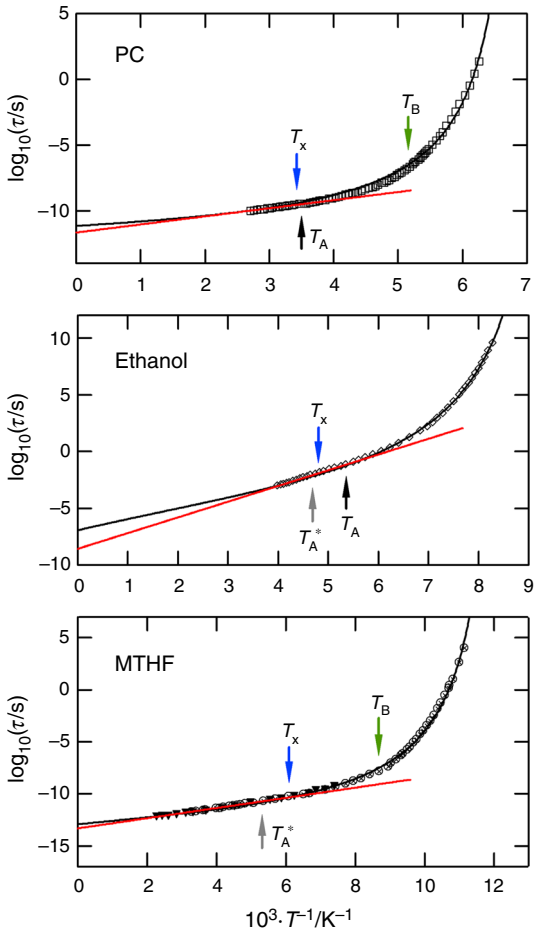

Fig. 4 Temperature dependence of $\log_{10}(\tau/s)$ for PC, ethanol and MTHF fitted with the BSCNF model given by Eq. (1). The experimental data of τ for MTHF is taken from Ref. [8], which contains data obtained from different techniques and sources (e.g., dielectric spectroscopy, depolarized light scattering, etc. For details, see Ref. [8]). The locations of the characteristic temperatures T_x, T_A, and T_B are shown, together with $T_A^* = 213$ K for ethanol [9] and $T_A^* = 189$ K for MTHF. The T_A^* of MTHF is determined following the observation given in Ref. [8]

activation energy calculated by the model, $E_\tau^{(\mathrm{BSCNF})}(T)$, is lower than E_∞ and becomes comparable to E_∞ around T_x. At ambient pressure, naturally, the description of liquid structural relaxation is valid only below the boiling point T_b [21]. Nevertheless, the result of Fig. 4 indicates that over the wide temperature range, the BSCNF model given by Eq. (1) is sufficiently acceptable in describing the non-Arrhenius structural relaxation behavior with the Arrhenius-like one at high temperatures. In Fig. 4, we have also indicated the inverse temperatures $10^3/T_A$ and $10^3/T_x$, which are denoted by black up-pointing arrow and blue down-pointing arrow, respectively. In the analyses of PC and MTHF, the inverse dynamic crossover temperature $10^3/T_B$ is denoted by green down-pointing arrow. For ethanol, the comparison with T_B is omitted, because the experimental data used here does not cover the reported value of T_B, for instance, $T_B = 111$ K [6] (or $10^3/T_B \approx 9\ \mathrm{K}^{-1}$). In Table 1, the values of T_x and T_A, and the reported T_A^*, are listed. As mentioned in the Introduction section, the objective of the present work was to compare T_x with T_A. From Fig. 4 it is confirmed that T_x is close to T_A, and higher than T_B. For ethanol, $T_x = 208$ K is closer to the reported value $T_A^* = 213$ K [9] which is denoted by gray up-pointing arrow. For MTHF, it is interesting to note that T_x is roughly at the transition point where the α-relaxation time data start to deviate from the Arrhenius-like pattern.

With the present results that T_x is close to T_A, it is inferred that the Arrhenius crossover phenomena can be linked to the low-temperature relaxation dynamics that occurs near the glass-transition range. From Eqs. (3) and (4), T_x is proportional to $|\Delta E||\Delta Z|/R$. As shown in our previous study [25], we already know that when the condition $|\Delta E|/E_0 = |\Delta Z|/Z_0$ is satisfied, Eq. (1) reduces analytically to the VFT-like expression. As a corollary of this result, the temperature defined by $T_F = |\Delta E||\Delta Z|/R$ becomes almost the same to the ideal glass-transition temperature, or the Vogel temperature T_0 in the VFT equation. In other words, according to the BSCNF model, the diverging behavior as described by the VFT-like description is ascribed to the binding energy distribution of the structural units. Furthermore, Eq. (4) indicates the relation $T_x \propto T_F \approx T_0$ for fragile systems. It is a well-known fact that the ideal glass-transition temperature T_0 is close to the Kauzmann temperature T_K, at which the extrapolated entropy of a supercooled liquid crosses that of the ordered crystal [45]. Thus, the present result suggests a possible link between the Arrhenius crossover behavior and the low-temperature relaxation dynamics. Concerning the relation between T_x and T_A for other fragile liquids, further verification is needed. But since our BSCNF model is applicable enough to the high-temperature transition from the Arrhenius-like relaxation behavior, the viewpoint discussed above will be useful in the study of vitrification in fragile systems.

Conclusions

In the present study, the Arrhenius temperature T_A and the cooperativity onset temperature T_x derived from the BSCNF model were directly compared by investigating the temperature dependence of α-relaxation time data. In order to specify T_A, we examined the variation in the averaged slope angle $\Delta\bar{\phi}(T)$. It was shown that based on the method explored, the transition from the Arrhenius-like relaxation behavior at high temperature to the non-Arrhenius-like one is unambiguously identified as shown in Figs. 2 and 3. The present method to evaluate T_A by using Eqs. (9)–(11) is based on the temperature derivation, which is analogous to the Stickel plot $f_\tau(T)$, but new efforts were made to highlight the Arrhenius crossover characteristics by using the averaging procedures explored. For the determination of T_x, the BSCNF model was applied to the α-relaxation time of PC, ethanol and MTHF, and was found to agree with the experimental data reasonably well in a wide temperature range. Namely, Eq. (1) is capable of describing qualitatively the change from an Arrhenius-like relaxation behavior to a non-Arrhenius relaxation in fragile liquids. The main objective of the present work was to confirm whether T_x is found close to T_A as expected from our recent work, which could lead to meaningful insights of vitrification in fragile liquids. The method of the analysis used here confirmed this point. In addition, it was also found that T_x is higher than T_B. Finally, in terms of the BSCNF model, a relation was presented that connects the high-temperature transition from the Arrhenius-like relaxation behavior to the low-temperature relaxation dynamics near the glass-transition range. As described in Eq. (4), it was given by $T_x \propto T_F = |\Delta E||\Delta Z|/R$ which is closely related with the ideal glass-transition temperature or the Vogel temperature T_0, as is shown in our previous study [25].

References

1. Angell CA. Relaxation in liquids, polymers and plastic crystals—strong/fragile patterns and problems. J Non Cryst Solids. 1991;131–133:13–31.
2. Angell CA, Green JL, Ito K, Lucas P, Richards BE. Glassformer fragilities and landscape excitation profiles by simple calorimetric and theoretical methods. J Therm Anal Calorim. 1999;57:717–36.
3. Novikov VN, Sokolov AP. Poisson's ratio and the fragility of glass-forming liquids. Nature. 2004;431:961–3.

4. Kokshenev VB. Characteristic temperatures of liquid–glass transition. Physica A. 1999;262:88–97.
5. Saiter A, Delbreilh L, Couderc H, Arabeche K, Schönhals A, Saiter J-M. Temperature dependence of the characteristic length scale for glassy dynamics: combination of dielectric and specific heat spectroscopy. Phys Rev E. 2010;81:041805.
6. Martinez-Garcia JC, Martinez-Garcia J, Rzoska SJ, Hulliger J. The new insight into dynamic crossover in glass forming liquids from the apparent enthalpy analysis. J Chem Phys. 2012;137:064501.
7. Popova VA, Surovtsev NV. Transition from Arrhenius to non-Arrhenius temperature dependence of structural relaxation time in glass-forming liquids: continuous versus discontinuous scenario. Phys Rev E. 2014;90:032308.
8. Schmidtke B, Petzold N, Kahlau R, Rössler EA. Reorientational dynamics in molecular liquids as revealed by dynamic light scattering: from boiling point to glass transition temperature. J Chem Phys. 2013;139:084504.
9. Popova VA, Malinovskii VK, Surovtsev NV. Temperature of nanometer-scale structure appearance in glasses. Glass Phys Chem. 2013;39:124–9.
10. Koštál P, Hofírek T, Málek J. Viscosity measurement by thermomechanical analyzer. J Non Cryst Solids. 2018;480:118–22.
11. Kondratiev A, Khvan AV. Analysis of viscosity equations relevant to silicate melts and glasses. J Non Cryst Solids. 2016;432:366–83.
12. Jaiswal A, Egami T, Kelton KF, Schweizer KS, Zhang Y. Correlation between fragility and the Arrhenius crossover phenomenon in metallic, molecular, and network liquids. Phys Rev Lett. 2016;117:205701.
13. Pan S, Wu ZW, Wang WH, Li MZ, Xu L. Structural origin of fractional Stokes–Einstein relation in glass-forming liquids. Sci Rep. 2017;7:39938.
14. Novikov VN. Connection between the glass transition temperature T_g and the Arrhenius temperature T_A in supercooled liquids. Chem Phys Lett. 2016;659:133–6.
15. Surovtsev NV. On the glass-forming ability and short-range bond ordering of liquids. Chem Phys Lett. 2009;477:57–9.
16. Saiter A, Couderc H, Grenet J. Characterisation of structural relaxation phenomena in polymeric materials from thermal analysis investigations. J Therm Anal Calorim. 2007;88:483–8.
17. Schröter K. Glass transition of heterogeneous polymeric systems studied by calorimetry. J Therm Anal Calorim. 2009;98:591–9.
18. Saiter JM, Grenet J, Dargent E, Saiter A, Delbreilh L. Glass transition temperature and value of the relaxation time at T_g in vitreous polymers. Macromol Symp. 2007;258:152–61.
19. Stickel F, Fischer EW, Richert R. Dynamics of glass-forming liquids. II. Detailed comparison of dielectric relaxation, dc-conductivity, and viscosity data. J Chem Phys. 1996;104:2043–55.
20. Schmidtke B, Petzold N, Pötzschner B, Weingärtner H, Rössler EA. Relaxation stretching, fast dynamics, and activation energy: a comparison of molecular and ionic liquids as revealed by depolarized light scattering. J Phys Chem B. 2014;118:7108–18.
21. Louzguine-Luzgin DV, Louzguina-Luzgina LV, Fecht H. On limitations of the viscosity versus temperature plot for glass-forming substances. Mater Lett. 2016;182:355–8.
22. Ikeda M, Aniya M. A measure of cooperativity in non-Arrhenius structural relaxation in terms of the bond strength–coordination number fluctuation model. Eur Polym J. 2017;86:29–40.
23. Aniya M. A model for the fragility of the melts. J Therm Anal Calorim. 2002;69:971–8.
24. Ikeda M, Aniya M. Correlation between fragility and cooperativity in bulk metallic glass-forming liquids. Intermetallics. 2010;18:1796–9.
25. Ikeda M, Aniya M. Understanding the Vogel–Fulcher–Tammann law in terms of the bond strength–coordination number fluctuation model. J Non Cryst Solids. 2013;371–372:53–7.
26. Lunkenheimer P, Kastner S, Köhler M, Loidl A. Temperature development of glassy α-relaxation dynamics determined by broadband dielectric spectroscopy. Phys Rev E. 2010;81:051504.
27. Jaiswal A, O'Keeffe S, Mills R, Podlesynak A, Ehlers G, Dmowski W, Lokshin K, Stevick J, Egami T, Zhang Y. Onset of cooperative dynamics in an equilibrium glass-forming metallic liquid. J Phys Chem B. 2016;120:1142–8.
28. Adichtchev SV, Surovtsev NV. Raman line shape analysis as a mean characterizing molecular glass-forming liquids. J Non Cryst Solids. 2011;357:3058–63.
29. Aniya M, Ikeda M. Sahara. A comparative study of molecular motion cooperativity in polymeric and metallic glass-forming liquids. Mater Sci Forum. 2017;879:151–6.
30. Huth H, Beiner M, Donth E. Temperature dependence of glass-transition cooperativity from heat-capacity spectroscopy: two post-Adam-Gibbs variants. Phys Rev B. 2000;61:15092–101.
31. Rijal B, Delbreilh L, Saiter J-M, Schönhals A, Saiter A. Quasi-isothermal and heat–cool protocols from MT-DSC. J Therm Anal Calorim. 2015;121:381–8.
32. Henricks J, Boyum M, Zheng W. Crystallization kinetics and structure evolution of a polylactic acid during melt and cold crystallization. J Therm Anal Calorim. 2015;120:1765–74.
33. Pawlus S, Kunal K, Hong L, Sokolov AP. Influence of molecular weight on dynamic crossover temperature in linear polymers. Polymer. 2008;49:2918–23.
34. Pawlus S, Mierzwa M, Paluch M, Rzoska SJ, Roland CM. Dielectric and mechanical relaxation in isooctylcyanobiphenyl (8*OCB). J Phys Condens Matter. 2010;22:235101.
35. Rijal B, Delbreilh L, Saiter A. Dynamic heterogeneity and cooperative length scale at dynamic glass transition in glass forming liquids. Macromolecules. 2015;48:8219–31.
36. Gotze W, Sjogren L. Relaxation processes in supercooled liquids. Rep Prog Phys. 1992;55:241–376.
37. Schönhals A. Evidence for a universal crossover behaviour of the dynamic glass transition. Europhys Lett. 2001;56:815–21.
38. Ndeugueu JL, Ikeda M, Aniya M. A comparison between the bond-strength–coordination number fluctuation model and the random walk model of viscosity. J Therm Anal Calorim. 2010;99:33–8.
39. Saiter A, Bureau E, Zapolsky H, Saiter JM. Cooperativity range and fragility in vitreous polymers. J Non Cryst Solids. 2004;345–346:556–61.
40. Arkhipov VI, Bässler H. Random-walk approach to dynamic and thermodynamic properties of supercoled melts. 1. Viscosity and average relaxation times in strong and fragile liquids. J Phys Chem. 1994;98:662–9.
41. Ngai KL. Dynamic and thermodynamic properties of glass-forming substances. J Non Cryst Solids. 2000;275:7–51.
42. Mirigian S, Schweizer KS. Elastically cooperative activated barrier hopping theory of relaxation in viscous fluids. II. Thermal liquids. J Chem Phys. 2014;140:194507.
43. Kivelson D, Tarjus G, Zhao X, Kivelson SA. Fitting of viscosity: distinguishing the temperature dependences predicted by various models of supercooled liquids. Phys Rev E. 1996;53:751–8.
44. Popova VA, Surovtsev NV. The limitation for popular descriptions of α-relaxation temperature dependence. arXiv:1104.2693v1 [cond-mat.mtrl-sci] http://arxiv.org/abs/1104.2693.
45. Kauzmann W. The nature of the glassy state and the behavior of liquids at low temperatures. Chem Rev. 1948;43:219–56.